



Lawrence Berkeley Laboratory

UNIVERSITY OF CALIFORNIA

EARTH SCIENCES DIVISION

RECEIVED
LAWRENCE
BERKELEY LABORATORY

APR 25 1986

Presented at the (SPE) Society of Engineers
56th Annual California Regional Meeting,
Oakland, CA, April 2-4, 1986

LIBRARY AND
DOCUMENTS SECTION

A MULTIPLE-POROSITY METHOD FOR SIMULATION
OF NATURALLY FRACTURED PETROLEUM RESERVOIRS

Y.-S. Wu and K. Pruess

February 1986

TWO-WEEK LOAN COPY

*This is a Library Circulating Copy
which may be borrowed for two weeks.*



LBL-21111

c.2

DISCLAIMER

This document was prepared as an account of work sponsored by the United States Government. While this document is believed to contain correct information, neither the United States Government nor any agency thereof, nor the Regents of the University of California, nor any of their employees, makes any warranty, express or implied, or assumes any legal responsibility for the accuracy, completeness, or usefulness of any information; apparatus, product, or process disclosed, or represents that its use would not infringe privately owned rights. Reference herein to any specific commercial product, process, or service by its trade name, trademark, manufacturer, or otherwise, does not necessarily constitute or imply its endorsement, recommendation, or favoring by the United States Government or any agency thereof, or the Regents of the University of California. The views and opinions of authors expressed herein do not necessarily state or reflect those of the United States Government or any agency thereof or the Regents of the University of California.

A Multiple-Porosity Method for Simulation of Naturally Fractured Petroleum Reservoirs

Yu-Shu Wu and Karsten Pruess, Earth Sciences Division, Lawrence Berkeley Laboratory, University of California, Berkeley, California 94720

Paper to be presented at the Society of Engineers 56th Annual California Regional Meeting, April 2-4, 1986, Oakland, California.

ABSTRACT

This paper describes the application of the method of "Multiple Interacting Continua" (MINC) to the simulation of oil recovery in naturally fractured reservoirs. A generalization of the double-porosity technique, the MINC-method permits a fully transient description of interporosity flow, using numerical methods. The method has been successfully applied in the past to geothermal reservoir and chemical transport problems.

In this paper, we present examples to demonstrate the utility of the MINC-method for modeling oil recovery mechanisms and field applications in fractured reservoirs. Specifically, results for water imbibition in individual matrix blocks obtained with the MINC method are compared with results from the conventional double-porosity method and with calculations using a detailed discretization of matrix blocks. The MINC-calculations are found to be accurate to better than 1 percent at all times, while double-porosity results can have large errors for matrix blocks of low permeability or large size. In addition, the MINC-method is used to match published results for five-spot waterfloods, and to study the coning behavior of a single well in the north China oil field. All results show that the MINC-method provides accurate predictions of the behavior of naturally fractured reservoirs, while requiring only a modest increase in computation work in comparison to the double-porosity method.

1. INTRODUCTION

The study of fluid flow in naturally fractured petroleum reservoirs has been a challenging task and has made considerable progress since the 1960's because many fractured hydrocarbon reservoirs have been discovered and put into development in the past decades. Most papers treating flow in fractured reservoirs consider that global flow occurs primarily

References and illustrations at end of paper.

through the high-permeability, low-effective-porosity fracture system surrounding matrix rock blocks. The matrix blocks contain the majority of the reservoir storage volume and act as local source or sink terms to the fracture system. The fractures are interconnected and provide the main fluid flow path to injection and production wells.^{1,2}

Due to the complexity of the pore structure of fractured reservoirs, there is no universal method for the simulation of reservoir behavior. Several different double-porosity models (DPM) have been developed to describe single-phase and multiphase flow in fractured media³⁻¹¹. Usually, analytical approximations are introduced for the coupling between fracture and matrix continua. For example, it is commonly assumed that a quasi-steady state exists in the primary-porosity matrix elements at all times.

Very little work has been done so far in studying transient flow in the matrix blocks or between matrix and fracture systems either numerically or experimentally. As a generalization of the double-porosity concept, Pruess and Narasimhan developed a "Multiple Interacting Continua" method (MINC)⁷, which treats the multiphase and multidimensional transient flow in both fractures and matrix blocks by a numerical approach. This method was successfully applied to a number of geothermal reservoir problems^{6,12,13}. The MINC-method of Pruess and Narasimhan⁷ involves discretization of matrix blocks into a sequence of nested volume elements, which are defined on the basis of distance from the block surface (Fig. 1a). In this way it is possible to resolve in detail the gradients (of pressure, temperature, etc.) which drive interporosity flow. This discretization technique was later adopted by Gilman¹¹ for flow in fractured hydrocarbon reservoirs, and by Neretnieks and Rasmuson¹⁴ for chemical transport in fractured groundwater systems.

In the present paper, we apply the MINC-method to study oil recovery mechanisms in fractured reservoirs, and to obtain insight into the behavior of water-oil flow during the

mechanism of oil production in waterflooding or waterconing of fractured reservoirs¹⁵. For multiphase flow, pressure, viscous, gravitational, and capillary forces should all be taken into account. In order to understand the roles played by the three kinds of forces, we have studied the imbibition process with the MINC method, the conventional double-porosity method, and with a detailed explicit discretization of matrix blocks. The comparison of the results from the three methods shows that the MINC-method can give an accuracy of better than one percent at all times, while the double-porosity approximation with quasi-steady interporosity flow can produce large errors, especially for matrix blocks with low permeability or large size.

We also apply the MINC-method to match published data of a five-spot water-flood^{4,9}, and the observed coning behavior of a well with bottom water drive in a fractured oil reservoir¹⁷. Satisfactory results have been obtained for the two examples. In both the imbibition study of individual matrix blocks and field-scale applications, the MINC-method is found to give more reliable history matching and behavior predictions for the simulation of fractured reservoir than the conventional double porosity method (DPM).

In most previous analytical or numerical studies of multiphase flow in porous media, it has been taken for granted that the matrix system can be treated as a single continuum with (locally) uniform pressure and fluid saturation distributions. To our knowledge, no studies have been published for multiphase flow about how much error will be introduced by this treatment, and under what conditions the quasi-steady approximation for interporosity flow is acceptable for engineering applications. The applicability of the DPM method is discussed by analyzing the results from individual block imbibition studies and field-scale examples with MINC and DPM in this paper. Through the work of this paper, it is found that the DPM method is often not suitable for the simulation of oil-water imbibition processes in naturally fractured reservoirs. Depending on reservoir fluid and rock properties, DPM may either overestimate or underestimate imbibition oil recovery from matrix blocks, especially for matrix blocks with low permeability and large size, or for high oil viscosity. In some special cases, the results from MINC and DPM calculations are very close either because of similarities in individual block response predicted from either method, or because of the compensatory effect of global flow in the fractures on individual block imbibition response in field-scale modeling. In general, it will be difficult to determine the suitability of DPM for a given reservoir problem. It is suggested that individual matrix imbibition studies be carried out with various possible reservoir parameters, using DPM approximation as well as explicit discretization, before applying DPM to actual reservoir simulation. Comparison between DPM and EDM results for individual matrix blocks may provide clues for the accuracy to be expected from the DPM approximation in field studies. When changes in water saturation in the fractures are rapid, as may often happen in coning problems, or in response to rate changes, it is usually necessary to account for the transient flow inside the matrix blocks, and between matrix and fractures.

2. MINC-METHOD

The method of "Multiple Interacting Continua" (MINC), a generalization of the double-porosity technique, is applicable

for numerical simulation of heat and multiphase fluid flow in multidimensional fractured porous media. The method permits treatment of multiphase fluids with large and variable compressibility, and allows for phase transitions with latent heat effects, as well as for coupling between fluid and heat flow. By dividing the matrix into subdomains, the transient interaction between matrix and fractures is treated in a realistic way. The numerical implementation of the MINC-method is most easily accomplished by means of an integral finite difference formulation¹⁸.

An important point of the MINC-method is the generation of computational grids²⁰. A fractured reservoir is at first partitioned into "primary" volume elements (or grid blocks), such as would usually be employed for a porous medium. The interblock flow connections are then assigned to the fracture continuum, and each primary grid block is sub-divided into a sequence of "secondary" nested volume elements, which are defined on the basis of distance from the matrix block surfaces (Fig. 1a). With these sub-continua it is possible to represent the transient flow in the matrix blocks, and transient interporosity flow between matrix and fractures. For problems involving strong gravity effects (e.g., gas injection), it is possible to define more general flow connections which allow for gravity drainage into fractures, and for global flow through matrix-matrix contacts.

The MINC-method contains the double-porosity approximation as a special case. It can be implemented simply by defining only one matrix continuum, and using an appropriate nodal distance for matrix-fracture flow (see Appendix A).

The simulations reported in this paper were carried out with a code "STMFLD1"*, which solves simultaneous mass balance equations for two hydrocarbon components and water, as well as a heat balance. STMFLD1 employs an integral finite difference technique for space discretization, and a fully implicit first-order time discretization. The resulting nonlinear algebraic equations are solved by Newton-Raphson iteration, using a sparse version of LU-decomposition for the set of linear equations arising at each iteration step¹⁹. STMFLD1 has a capability for simulating thermally enhanced oil recovery in fractured reservoirs, but was in the present work used only for isothermal oil-water two phase flow.

3. IMBIBITION OIL RECOVERY

Imbibition displacement of oil by water in relatively tight matrix blocks is a basic oil recovery mechanism in fractured reservoirs, owing to the fact that most of the oil in place is present in the low permeability matrix system, and flows into the fracture system under viscous, gravity and capillary forces during oil production. Detailed simulations of individual matrix blocks surrounded by water and oil are presented in this section to study oil recovery mechanisms and to demonstrate the validity of the MINC-method. The MINC results are compared with predictions from double-porosity and explicit-discretization methods (DPM and EDM; see Figs. 1b and 1c). Two kinds of matrix blocks, cubic and cylindrical, are modeled, and similar results are obtained. Relative permeability and capillary pressure data, and other parameters used are shown in Tables 1, 2 and 3.

*developed by K. Pruess

RESULTS

EDM is used as a comparison standard for MINC and DPM because EDM can take into account all the mechanisms, viscous, gravity and capillary effects. Figure 2 shows a schematic profile of a matrix block of cylindrical shape for MINC and EDM calculations.

Oil recovery versus time is shown in Figures 3a, 4a, and 5a, calculated from MINC, DPM and EDM for the three data sets given in Tables 1, 2, and 3. In Figure 6 we present oil recovery results for a cubic matrix block, using the data set of Thomas et al.⁹ This is virtually identical to the results for a cylindrical block, given in Figure 4a. After many calculations with various matrix sizes and parameters, we have found that there is almost no difference in flow behavior between cubic and cylindrical matrix blocks.

Comparing the oil recovery calculated by the three methods, it can be found that the MINC-method is accurate enough to simulate the water-oil imbibition process, while the DPM approach can give very large errors because it neglects transient flow in the matrix. In all cases we have studied, there is excellent agreement between the MINC and EDM results. It is interesting to note that the MINC-method requires only a modest increase in computational work in comparison to DPM because of the one-dimensional treatment of flow in the matrix, and saves much more computer time and storage than EDM.

As shown in Figures 3-6, there is a large difference in oil recovery between the MINC (or EDM) and DPM results. From the curve of imbibition rates (flow rate of oil from matrix into fractures) versus time in Figures 3b, 4b and 5b the cause of the difference is apparent. The imbibition rates are quite different between the two methods at early time, because DPM underestimates the capillary gradient near the matrix block surface. In fact, in DPM the initial differences in capillary pressures between matrix and fractures are assumed to occur over a quasi-steady flow distance D , which is much larger than the nodal distance we employ for the first matrix continuum in the MINC-method (see Appendix A). Subsequently the MINC-method predicts a buildup of water saturation near the matrix block surface, which diminishes the capillary pressure gradient driving interporosity flow, as well as oil relative permeability. This results in a steeper decline in imbibition rate than that predicted from the DPM approximation, in which all saturation changes are averaged over the entire matrix block. Therefore, at intermediate times, DPM overpredicts imbibition rates. Eventually, for very large times, the DPM imbibition rates decline below the MINC-predictions. This occurs simply because for $t \rightarrow \infty$ all approximations must converge to the the same total oil recovery, corresponding to attainment of capillary equilibrium between matrix and fractures. The relative lengths of the "early", "intermediate", and "late" time period, and the magnitude of deviation between MINC and DPM, depend on formation parameters, PVT properties, and initial conditions.

The agreement between MINC and EDM is excellent throughout. This is further substantiated in Figure 7, which compares the water saturations calculated in MINC approximation for a certain distance from the surface of a cylindrical block (see Fig. 2) with the detailed predictions of EDM. It is

seen that the MINC-method underpredicts water saturations near the "corners", where imbibition effects through the cylinder mantle overlap with those through the upper (or lower) cylinder surface. Away from the corners, imbibition effects are slightly overpredicted by the MINC-method. The deviations are such that the saturations computed in MINC-approximation agree extremely well with the average saturation at a given distance from the block surface obtained in EDM. Figure 7 shows that this holds true even when gravity effects are included, as long as saturations are uniform over the block surface. This result confirms a theoretical prediction by Pruess²⁰.

Effects of Matrix Block Size and Permeability

In Appendix B we show that, as far as interporosity flow is concerned, a change in linear matrix block size by a factor α is equivalent to a change in block permeability by a factor $1/\alpha^2$, provided gravity effects are small in comparison to capillary effects. We have verified this by comparing calculations for cylindrical and cube-shaped matrix blocks of widely different permeability and size. This result makes it possible to plot imbibition oil recovery in terms of a dimensionless time t_D , which is proportional to $(k/L^2)t$ (see Figure 8).

One of the most difficult problems in history matching and performance prediction of fractured reservoirs is to determine the matrix block size because it cannot be measured directly, so that the parameter usually has to be established after tedious history-matching calculations. The equivalence between changes in matrix block size and permeability facilitates practical application of the MINC-method to actual reservoir problems and history matching. A computational grid for a MINC-model of a flow system needs to be generated only once for a given matrix block shape; changes in matrix block sizes can then be implemented simply by appropriate adjustments in matrix permeability.

The same holds true when considering not just one kind of block shape, but a distribution of block shapes and sizes, based on some stochastic fracture distribution. As was shown by Pruess and Karasaki²¹, the effective shape of a distribution of block sizes can be conveniently represented by means of a "proximity function" $PROX(x)$, which represents the fraction of matrix material present within a distance x from the fractures. Knowledge of the proximity function is sufficient for defining all geometric parameters of a computational grid in the MINC-method. Based on the discussion of Appendix B it is clear that scaling of all matrix block dimensions in any distribution of shapes and sizes by a factor α will be equivalent to a change in matrix block permeability by a factor $1/\alpha^2$ (provided gravity effects in interporosity flow are small).

4. A FIVE-SPOT EXAMPLE

In order to demonstrate the application of the MINC-method to a field-scale problem, we present a comparison with previous calculations of Kazemi et al.⁴ and Thomas et al.⁹ for five-spot waterflood. In this problem water is injected into one-quarter of a five-spot pattern at a rate of 200 STB/D, and the production rate of total liquid is set at 210 STB/D. Reservoir dimensions and properties are given in Table 4.

For the treatment of the flow between matrix and fractures, Warren and Root² have derived an equation for the shape factor σ for single-phase flow, based on the quasi-steady flow assumption,

$$\sigma = \frac{4N(N+2)}{L^2} \quad (4-1)$$

Where N is number of normal sets of fractures; ($N = 1, 2$ or 3), and

$$L = \begin{cases} L_x & \text{for } N = 1 \\ 2L_xL_y/(L_x+L_y) & \text{for } N = 2 \\ 3L_xL_yL_z/(L_xL_y+L_yL_z+L_zL_x) & \text{for } N = 3 \end{cases} \quad (4-2)$$

Kazemi et al. and Thomas et al. both employed the quasi-steady approximation, introduced by Warren and Root, and gave different formulae for the matrix shape factor σ . Kazemi et al. proposed,

$$\sigma = 4 \left(\frac{1}{L_x^2} + \frac{1}{L_y^2} + \frac{1}{L_z^2} \right) \quad (4-3)$$

and Thomas et al. suggested

$$\sigma = \frac{A}{LV_m} \quad (4-4)$$

It should be noticed that the shape factors calculated from the three equations above for a cubic matrix block are quite different. As mentioned in the previous sections, the matrix block size makes a difference in flow behavior of imbibition oil displacement, and so does the shape factor since it is related closely to the matrix block size. The simulation results for different σ may lead to remarkable differences in the performance prediction.

In the present five-spot example, Kazemi et al. used a value of $\sigma = 0.08^4$, which according to Equation (A.5) corresponds to a nodal distance of $D = 5.833$ ft. A comparison of our simulated water-oil ratios with the results of Kazemi et al. and Thomas et al.⁹ is shown in Figure 9. For the first two years, our calculation using $\sigma = 0.08$ is in excellent agreement with the curves of Kazemi et al. and Thomas et al., and shows slight deviations at later time. The curve for $\sigma = 0.36$ in Figure 9, based on Warren and Root's shape factor, is lower for the first three years, and has a more rapid increase during the later production period. We also carried out a MINC-calculation for this problem, using a discretization of five continua. Surprisingly, the results for produced water-oil ratio turned out to be virtually indistinguishable from those obtained in double-porosity approximation with $\sigma = 0.36$, even though over much of the five-spot pattern the saturation distributions are quite different in both cases. How can a transient and a quasi-steady approximation for interporosity flow, which give substantially different imbibition response for individual matrix blocks (compare Fig. 3a), end up yielding nearly indistinguishable water-oil ratios in a five-spot flood? The answer is that the aggregate response of many matrix blocks in a flood problem tends to compensate for differences in individual block response. In the present case, the double-porosity approximation gives more rapid oil recovery from an individual block over virtually the entire time period of interest (see Fig. 3a). Therefore, in the double-porosity calculation matrix

blocks near the injector will take up more water and deliver more oil than predicted from the MINC-method, so that blocks further downstream from the injector will "see" more oil and less water in the fractures. Therefore, those more distant blocks will give smaller imbibition rates. From this consideration it is clear that there will be a general tendency for aggregate effects of blocks to compensate for differences in individual block response. The fact that this compensation is virtually quantitative in the present case is to be considered fortuitous.

5. A CONING PROBLEM

In this section, the MINC approximation is used to match the observed coning behavior of a well in the north China oil field. The data have been previously analyzed by Chen whose basic reservoir model is axially symmetric, the symmetry axis coincides with the well. The upper part of the reservoir is the oil zone, the middle is the transition zone, and the lower part is the water zone. Near the top of the water zone there is a horizontal thin impervious break. The bottom water is supplied from the lowest surface of the cylinder on which the pressure is maintained at a constant value. The top and the external border of the cylinder are sealed - i.e., there is no flow across the boundaries. The data used are shown in Table 5.

As given in Table 5, Chen used $\sigma = 0.1068$, which corresponds to a cubic matrix block with $L = 23.7$ ft. In the history match simulation, parameters are calibrated from the water-cut data of the first 200 days of production, and the water-cut data after 200 days are used for checking the predicted results.

The results of the history matching and the behavior prediction are shown in Figure 10, computed by MINC and DPM from the data of Table 5, respectively. Both models give a reasonable match for observed performance; differences between DPM and MINC are small in this case.

6. ON THE VALIDITY OF THE DOUBLE-POROSITY METHOD (DPM)

For practical simulation applications it would be preferable to use the simpler DPM approximation whenever possible, and to resort to the more complex MINC-description only in cases where the accuracy of DPM is poor. In this section we examine in more detail the conditions for which acceptable accuracy can be attained with the DPM method. The limitations of DPM can be seen best when comparing the temporal evolution of imbibition rates in individual matrix blocks with the more accurate MINC-prediction. As was discussed above, one can distinguish three time periods (see also Figures 11b, 13b, 14b):

- (1) an early period, in which DPM underpredicts imbibition rate, because it underpredicts the capillary gradients at the matrix block surface;
- (2) an intermediate period, in which DPM overpredicts imbibition rate, because it underestimates buildup of water saturation near the matrix block surface; and

- (3) a late time period, in which DPM again underpredicts imbibition rate, because in the intermediate time period (2) the block has moved closer towards eventual capillary equilibrium with the fractures than would be predicted from MINC.

The relative lengths of these time periods, and the magnitude of deviation between DPM and MINC in them, depend upon formation and fluid properties. Generally speaking, differences tend to be larger (DPM less accurate) for small matrix permeability, large matrix block dimensions, large matrix porosity, or large oil viscosity. This can be seen by comparing the imbibition results obtained for Chen's data¹⁷ (Figures 10-11) with those calculated for a modified data set, in which matrix permeability was decreased from 5 and for 0.1 md, and porosity was increased from 5 percent to 20 percent (Figure 12-13). For the original data of Chen most matrix blocks are in the "intermediate" time period (2) during the water coning process with relatively minor differences between DPM and MINC (see Figure 11b). For the modified data most matrix blocks are in time period (1) (see Figure 13b), with very large differences between DPM and MINC.

Reservoir response is in general more complicated than individual block response, because it involves a superposition of effects from many matrix blocks. Depending upon their location in the reservoir relative to the water table, and to injection and production wells, different blocks will be at different periods of the imbibition "cycle". Aggregate imbibition response of many blocks in a reservoir may be similar in DPM and MINC, even if individual block responses are rather different. This behavior was observed in our simulations of Kazemi's five spot waterflood example, where DPM and MINC gave virtually indistinguishable results even though individual block response predicted from DPM differs considerably from the MINC results (Figures 14a, 14b). The explanation here is that with time the matrix blocks near the injector move into stages (2) or (3) of the imbibition cycle, while the blocks closer to the production well remain in stage (1) for a longer time. Overall reservoir response then tends to average out the differences existing in each stage.

For practical reservoir simulation problems, it would be desirable to be able to evaluate the accuracy to be expected from DPM without actually going through a reservoir-wide MINC-calculation as well. It may be possible to accomplish this by plotting individual block imbibition data as shown in Figure 15. Here we have shown the ratio of recovery predictions from MINC and DPM as a function of total recovery. This presentation of the data removes the somewhat spurious dependence on real (physical) time, instead emphasizing the connection between total recovery and accuracy of DPM. (Note that an explicit discretization calculation for an individual block could be used instead of the MINC-calculation, with virtually indistinguishable results.) Figure 15 shows why DPM for the modified data of Chen strongly underestimates oil recovery (overestimates WOR): all matrix blocks are in conditions that plot above $OR_M/OR_D = 1$. For Chen's original data, as well as for Kazemi's data, the OR_M/OR_D ratio reaches 1 for substantially smaller oil recovery. In these cases, therefore, some matrix blocks will have $OR_M/OR_D > 1$ while others will have $OR_M/OR_D < 1$ after a relatively modest recovery

period. In this situation differences in individual block response will tend to average out, giving a favorable situation for applying DPM.

7. CONCLUSIONS

1. The conventional double-porosity method can give large errors for simulation of oil recovery from individual matrix blocks or from a reservoir by water-oil imbibition mechanisms. The errors increase rapidly with enlargement of matrix blocks or fluid viscosity, and with decrease in rock permeability.

2. The method of "multiple interacting continua" (MINC) takes into account the transient flow of fluids both in the matrix system and in the fractures. Comparisons with calculations using a detailed explicit discretization of matrix blocks have shown that the MINC-method gives accurate predictions for water imbibition.

3. Results of five-spot waterflood and coning simulations indicate that the aggregate response of many matrix blocks in a reservoir has a general tendency to compensate for differences in individual block response. This suggests that the double-porosity method with quasi-steady approximation for interporosity flow may be applicable even in cases where its basic assumptions are poorly justified.

4. An estimation of the suitability of the double-porosity approximation for water flooding and coning problems can be obtained by comparing quasi-steady and transient imbibition predictions for individual matrix blocks.

NOMENCLATURE

A	interface area of matrix block, [L ²]
A _{nm}	interface area between volume elements n and m, [L ²]
b	formation volume factor, [L ³ /L ³]
c	compressibility, [Lt ² /M]
D	distance between nodal points, [L]
D _j	nodal distance for the innermost matrix node, [L]
F	mass flux, [M/L ² ·t]
h	time level index
k	absolute matrix permeability, [L ²]
k	component index (k = oil, water), [L ²]
k _β	relative permeability to the β-phase
L	characteristic dimension of matrix block, [L]
L _x	matrix block length, [L]
L _y	matrix block width, [L]
L _z	matrix block height, [L]
M	accumulation term in mass balance equation, [M/L ³]
P	pressure, [M/L·t ²]
P _{cwo}	capillary pressure, [M/Lt ²]
S	saturation
t	time, [t]
V _m	matrix-block volume, [L ³]

V_n	volume of grid block n, [L ³]
X	mass fraction
α	scale factor (Appendix A)
μ	viscosity, [M/Lt]
ρ	mass density of fluid, [M/L ³]
σ	matrix shape factor, [L ⁻²]
ϕ	porosity

Subscripts

b	bubble point
f	fracture
m	matrix
n	index number of volume element
o	oil
w	water
β	phase

ACKNOWLEDGEMENT

This work was supported, in part, by the Ministry of Education, The Peoples Republic of China, and the U.S. Department of Energy under Contract No. DE-AC03-76SF00098.

REFERENCES

- Barenblatt, G. E., Zheltov, I. P. and Kochina, I. N.: "Basic Concepts in the Theory of Seepage of Homogeneous Liquids in Fissured Rocks," *J. Appl. Math.*, (USSR), Vol. 24, No. 5, (1960) 1286-1303.
- Warren, J. E., and Root, P. J.: "The Behavior of Naturally Fractured Reservoirs," *Soc. Pet. Eng. J.*, (Sept. 1963) 245-255, Trans. AIME, Vol. 228.
- Kazemi, H.: "The Behavior of Naturally Fractured Reservoirs with Uniform Fractured Distribution," *Soc. Pet. Eng. J.*, (Dec. 1969) 451-462, Trans., AIME, Vol. 246.
- Kazemi, H., Merrill, L. S., Porterfield, K. L., and Zeman, P. R.: "Numerical Simulation of Water-Oil Flow in Naturally Fractured Reservoirs," *Soc. Pet. Eng. J.*, (Dec. 1976) 317-326.
- Duguid, I. O., and Lee, P. C.: "Flow in Fractured Porous Media," *Water Resources Res.*, Vol. 13, No. 3, (1977) 558-566.
- Pruess, K., and Narasimhan, T. N.: "On Fluid Reserves and the Production of Superheated Steam from Fractured, Vapor-Dominated Geothermal Reservoirs," *J. of Geo. Res.*, Vol. 87, No. B11, (1982) 9329-9339.
- Pruess, K., and Narasimhan, T. N.: "A Practical Method for Modeling Fluid and Heat Flow in Fractured Porous Media," Paper SPE 10509 Presented at the Sixth SPE-Symposium on Reservoir Simulation, New Orleans, LA, February 1982, *Soc. Pet. Eng. J.*, Vol. 25, No. 1, (Feb. 1985) 14-26.
- Pruess, K.: "A Quantitative Model of Vapor-Dominated Geothermal Reservoirs as Heat Pipes in Fractured Porous Rock," *Trans., Geothermal Research Council*, Vol. 9, Part II, (1985) 353-361.
- Thomas, L. K., Dixon, T. N., and Pierson, R. G.: "Fractured Reservoir Simulation," Paper SPE 9305 Presented at SPE-AIME 55th Annual Fall Meeting, Dallas, Texas, (Sept. 1980) 21-24.
- Gilman, J. R., and Kazemi, H.: "Improvements in Simulation of Naturally Fractured Reservoir," *Soc. Pet. Eng. J.*, (Dec. 1976) 317-326.
- Gilman, J. R.: "Numerical Simulation of Phase Segregation in the Primary Porosity (Matrix Blocks) in Two-Porosity Porous Media," Paper SPE 12272, Presented at SPE-Symposium on Reservoir Simulation, San Francisco, CA (Nov. 1983).
- Pruess, K.: "Heat Transfer in Fractured Geothermal Reservoirs with Boiling," *Water Resources Res.*, Vol. 19, No. 1, (Feb. 1983) 201-208.
- Bodvarsson, G. S., Pruess, K., and O'Sullivan, M. J.: "Injection and Energy Recovery in Fractured Geothermal Reservoirs," *Soc. Pet. Eng. J.*, Vol. 25, No. 2, (April 1985) 303-312.
- Neretnieks, I., and Rasmuson, A.: "An Approach to Modeling Radionuclide Migration in a Medium with Strongly Varying Velocity and Block Sizes Along the Flow Path," *Water Resources Res.*, Vol. 20, No. 12, (Dec. 1984) 1823-1836.
- De Swaan, A.: "Theory of Waterflooding in Fractured Reservoirs," *Soc. Pet. Eng. J.*, (April 1978) 117-122.
- Menovar, H., and Knapp, R. M.: "Numerical Simulation of the Imbibition Process in Fractured Reservoir," Paper SPE 9370 Presented at the SPE-AIME 55 Annual Fall Technical Conference and Exhibition, Dallas, TX (Sept. 1980).
- Chen, Huan-Zhang: "Numerical Simulation of Coning Behavior of a Single Well in a Naturally Fractured Reservoir," *Soc. Pet. Eng. J.*, (Dec. 1983) 879-884.
- Narasimhan, T. N., and Witherspoon, P. A.: "An Integrated Finite Difference Method for Analyzing Fluid Flow in Porous Media," *Water Resources Res.*, Vol. 12, No. 1, (1976) 57-64.
- Duff, I. S.: "MA28 - A Set of FORTRAN Subroutines for Sparse Unsymmetric Linear Equations," AERE Harwell Report R8730 (July 1977).
- Pruess, K.: "GMINC-A Mesh Generator for Flow Simulation in Fractured Reservoirs," Lawrence Berkeley Laboratory LBL-15227, Berkeley, CA (March 1983).
- Pruess, K., and Karasaki, K.: "Proximity Functions for Modeling Fluid and Heat Flow in Reservoirs with Stochastic Fracture Distributions," Presented at the Eighth Workshop on Geothermal Reservoir Engineering, Stanford University, Stanford, CA (Dec. 1982).

Appendix A: Relationship Between Double-Porosity Matrix Shape Factor and Geometric Parameters of the Integral Finite Difference Method.

Warren and Root (1963) wrote a quasi-steady approximation for interporosity flow in single phase conditions as follows:

$$\phi_m c_m \frac{\partial \bar{p}_m}{\partial t} = \sigma \frac{k_m}{\mu} (\bar{p}_r - \bar{p}_m) \quad (\text{A.1})$$

The bars indicate averages over matrix and fracture continua, respectively. The parameter σ (Warren and Root used the notation α) is a "matrix shape factor" (Thomas et al., 1983); which characterizes the matrix block surface area per unit volume.

To obtain the relationship between σ and the geometric parameters used in an integral finite difference description of interporosity flow, consider the point differential equation for flow in the matrix blocks

$$\phi_m c_m \frac{\partial p_m}{\partial t} = \text{div} \frac{k_m}{\mu} \nabla p_m \quad (\text{A.2})$$

Integrating over one matrix block we obtain:

$$V \phi_m c_m \frac{\partial \bar{p}_m}{\partial t} = A \frac{k_m}{\mu} (\nabla p_m)_{\text{surface}} \quad (\text{A.3})$$

In double-porosity approximation (two continua), the pressure gradient at the block surface is approximated by the following finite difference expression

$$(\nabla p_m)_{\text{surface}} \approx \frac{\bar{p}_r - \bar{p}_m}{D} \quad (\text{A.4})$$

with D being the distance of the matrix nodal point from the block surface. Comparing Eqs. (A.1), (A.3) and (A.4), we obtain

$$\sigma = \frac{A}{VD} \quad (\text{A.5})$$

For matrix blocks in the shape of cubes, Warren and Root give $\sigma = 60/L^2$. Noting that $A/V = 6/L$ in this case, we obtain a nodal distance $D = L/10$ for quasi-steady flow. Different values of σ which have been proposed for multi-phase flow can be accommodated in the integral finite difference representation by simply calculating the corresponding nodal distance D from Eq. (A.5).

Appendix B: Dependence of Interporosity Flow on Matrix Block Size

Let us consider a scale change for the matrix blocks in which all distances between points change by the same common factor

$$l \rightarrow l' = \alpha l \quad (\text{B.1})$$

Such a scale change will not affect the shape of the blocks. In order to evaluate its effect on interporosity flow, we consider the governing mass balance equations for matrix-matrix or matrix-fracture flow. Ignoring gravity effects, we have

$$M_n^{k,h+1} - M_n^{k,h} - \frac{\Delta t}{V_n} \sum_m A_{nm} F_{nm}^k = 0 \quad (\text{B.2})$$

where

$$F_{nm}^k = \frac{k}{D_{nm}} \sum_{\beta} X_{\beta}^k \frac{k_{\beta}}{\mu_{\beta}} \rho_{\beta} (P_{\beta,m} - P_{\beta,n}) \quad (\text{B.3})$$

Thus, the permeability and geometry parameters appear in (B.2) in the group

$$k \frac{A_{nm}}{V_n D_{nm}} \quad (\text{B.4})$$

Suppose that the total number of matrix blocks in grid block V_n is ν . Under the scale change (B.1) this number will change to $\nu' = \nu/\alpha^3$. The surface area per matrix block will change from A_{nm}/ν to $\alpha^2 A_{nm}/\nu$, so that the total surface area will become

$$A_{nm}' = \nu' \frac{\alpha^2 A_{nm}}{\nu} = \frac{1}{\alpha} A_{nm} \quad (\text{B.5})$$

All nodal distances in the matrix will change according to

$$D_{nm}' = \alpha D_{nm} \quad (\text{B.6})$$

Note that for a matrix-fracture connection the same equation holds, because the fracture nodal point will be on the block surface, so that the entire group (B.4) will change as follows:

$$k \frac{A_{nm}'}{V_n D_{nm}'} = \frac{k}{\alpha^2} \frac{A_{nm}}{V_n D_{nm}} \quad (\text{B.7})$$

Thus, an increase in linear matrix block size by a factor α is equivalent to a reduction in matrix permeability by a factor α^2 . This result holds for arbitrary (fixed) block shapes, and in fact for arbitrary distributions of block sizes. Nowhere in the above discussion did we need to require matrix block sizes to be identical.

When gravity effects are included no simple block size-permeability relationship is possible. For a gravity term in F_{nm}^k , the geometric data would appear in the group

$$k \frac{A_{nm}}{V_n} \rightarrow k \frac{A_{nm}'}{V_n} = \frac{k}{\alpha} \frac{A_{nm}}{V_n}$$

For gravity contribution to flow, an increase in linear matrix block size by a factor α is equivalent to a decrease in permeability by the same factor. As matrix block sizes increase, therefore, the contribution of pressure forces to flow will diminish more rapidly than the contribution of gravity forces. This indicates that gravity forces may often be unimportant for imbibition in small matrix blocks, but may be very important for large matrix blocks.

Table 1.
Relative Permeabilities and Capillary Pressures
for Data Set 1 (Kazemi et al., 1976)

S_w	k_{rnf}	k_{rof}	P_{cwof} (psi)	k_{rwm}	k_{rom}	P_{cwom} (psi)
0.000	0.000	1.000	4.000	-	-	-
0.100	0.050	0.770	1.850	-	-	-
0.200	0.110	0.587	0.900	-	-	-
0.250	0.145	0.519	0.725	0.000	0.920	4.000
0.300	0.180	0.450	0.550	0.020	0.705	2.950
0.400	0.260	0.330	0.400	0.055	0.420	1.650
0.500	0.355	0.240	0.290	0.100	0.240	0.850
0.600	0.475	0.173	0.200	0.145	0.110	0.300
0.700	0.585	0.102	0.160	0.200	0.000	0.000
0.800	0.715	0.057	0.110	-	-	-
0.900	0.850	0.021	0.050	-	-	-
1.000	1.000	0.000	0.000	-	-	-

Table 2
Parameters for Data Set 2 (Thomas et al., 1983)

S_w	Relative Permeability		P_{cwo} (psi)
	k_{rw}	k_{row}	
0.200	0.000	1.000	50.00
0.250	0.005	0.860	9.000
0.300	0.010	0.732	2.000
0.350	0.020	0.600	0.500
0.400	0.030	0.492	0.000
0.450	0.045	0.392	-0.40
0.500	0.060	0.304	-1.20
0.600	0.110	0.154	-4.00
0.700	0.185	0.042	-10.0
0.750	0.230	0.000	-40.0

Original bubble point, psig	5,545
Slope of b_o above P_b , vol/vol-psi	0.000012
Density of stock-tank oil, lbm/cu ft	51.14
Slope of the μ_o above P_b , cp/psi	0.0000172
Gas density at standard conditions, lbm/cu ft	0.058
Water formation volume factor, psig	1.07
Water compressibility, vol/vol-psi	$3.5 (10^{-6})$
Water viscosity, cp	0.35
Water density at standard conditions lbm/cu ft	65
Matrix compressibility vol/vol psi	$3.5 (10^{-6})$
Fracture compressibility, vol/vol psi	$3.5 (10^{-6})$
Matrix permeability, md	1
Matrix porosity, %	30

Table 3
Parameters for Data Set 3 (Southern California Oil Field)

S_w	Relative Permeability		P_{cwom} (psi)
	k_{rwm}	k_{rom}	
0.000	1.000	0.000	356.66
0.037	0.850	0.000	141.69
0.040	0.840	9.42E-11	124.26
0.049	0.811	2.41E-8	105.77
0.059	0.779	2.72E-7	88.27
0.073	0.735	1.95E-6	70.85
0.095	0.671	1.32E-5	53.42
0.099	0.659	1.72E-5	51.77
0.133	0.568	9.85E-5	35.92
0.201	0.411	8.41E-4	21.54
0.259	0.303	2.82E-3	14.38
0.351	0.173	1.13E-2	7.155
0.380	0.142	1.61E-2	5.668
0.455	0.0786	3.55E-2	3.082
0.554	0.0285	8.31E-2	1.643
0.624	0.0104	0.138	1.232
0.800	0.000	0.405	0.872
0.900	0.000	0.677	0.730
1.000	0.000	1.000	0.206

Matrix porosity (%)	20
Matrix Permeability, md	1
Fracture permeability, md	10,000
Rock compressibility vol/vol-psi	3×10^{-5}
Initial oil saturation	0.60
Oil density, lbm/cu ft	60.99
Oil viscosity, cp	90

Table 4
Data for Five-Spot Problem of Kazemi et al. (1976)

Initial Pressure, psia	3,959.89
Thickness, ft	30
Grid dimensions	8 x 8
Grid spacing, $\Delta x = \Delta y$ (ft)	75
Fracture porosity (%)	1
Matrix porosity (%)	19
Fracture permeability (effective), md	500
Matrix permeability, md	1
Matrix shape factor, sq ft ⁻²	0.08
Water compressibility, vol/vol-psi	$3.03(10^{-6})$
Bubble point pressure, psia	0
Water and oil formation volume factor at the bubble point, RB/STB	1.0
Slope of b_o above P_b , vol/vol-psi	0.0000103093
Fracture compressibility, vol/vol-psi	$3(10^{-6})$
Water viscosity, cp	0.4444
Water density, psi/cu ft	0.3611
Water injection rate, STB/D	200
Total production rate, STB/D	210

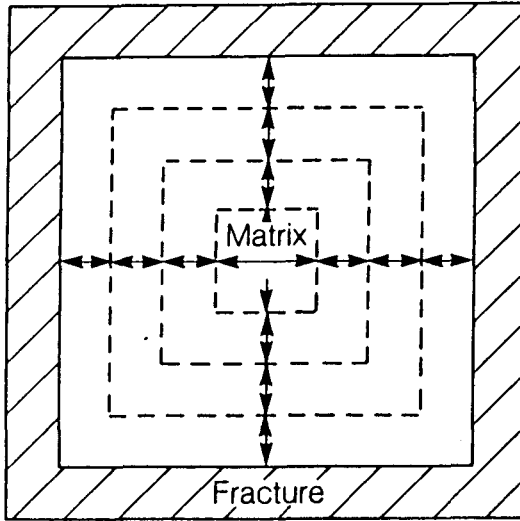
Table 5
Parameters for the Coning Problem
(Chen, 1983)¹⁷

Relative Permeability							
Fracture				Matrix			
S_w	k_{rw}	k_{ro}	P_c	S_w	k_{rw}	k_{ro}	P_c
0.0	0.0	1.0	3.869	0.280	0.0	0.940	3.869
0.1	0.052	0.764	1.906	0.324	0.016	0.705	2.773
0.2	0.111	0.592	0.896	0.368	0.034	0.544	2.077
0.3	0.182	0.439	0.540	0.412	0.052	0.431	1.579
0.4	0.271	0.328	0.370	0.456	0.070	0.348	1.195
0.5	0.367	0.239	0.277	0.500	0.092	0.276	0.868
0.6	0.470	0.163	0.205	0.544	0.113	0.207	0.612
0.7	0.586	0.103	0.135	0.588	0.131	0.149	0.384
0.8	0.715	0.057	0.085	0.632	0.154	0.092	0.213
0.9	0.854	0.017	0.043	0.676	0.178	0.034	0.085
1.0	1.0	0.0	0.0	0.720	0.200	0.0	0.0

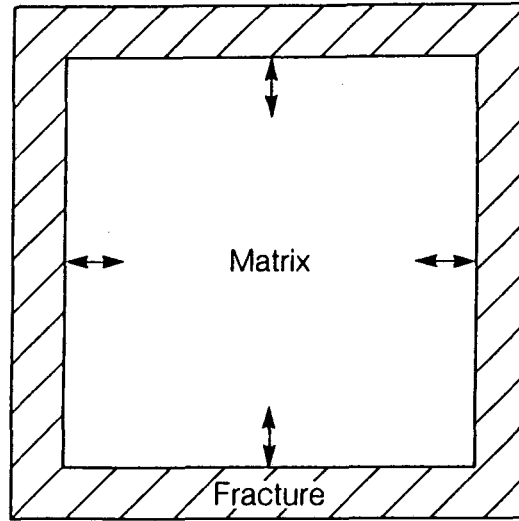
Perforated thickness, ft	68.2
Thickness of oil zone, ft	369.1
Thickness of water zone, ft	984.2
Well radius, ft	0.328
Well drainage radius, ft	984.2
Radius of the impervious break, ft	439.6

	Fracture	Matrix
Porosity	0.008	0.05
Permeability, md	3,500	5
Compressibility, psi^{-1}	0.0056	0.0
Vertical/horizontal permeability ratio	0.55	
Matrix shape factor sq ft^{-1}		0.1068

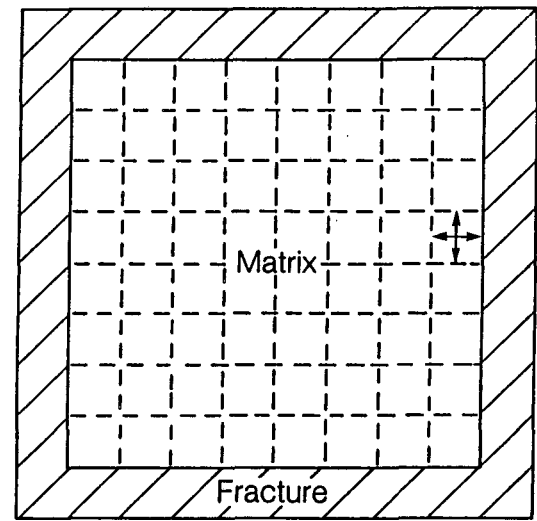
	Oil	Water
Viscosity, cp	15.8	0.3
Specific gravity	0.8456	1.02
Compressibility, psi^{-1}	0.000004	0.0
Formation volume factor, RB/STB	1.053	1.0



XBL 8512-12639

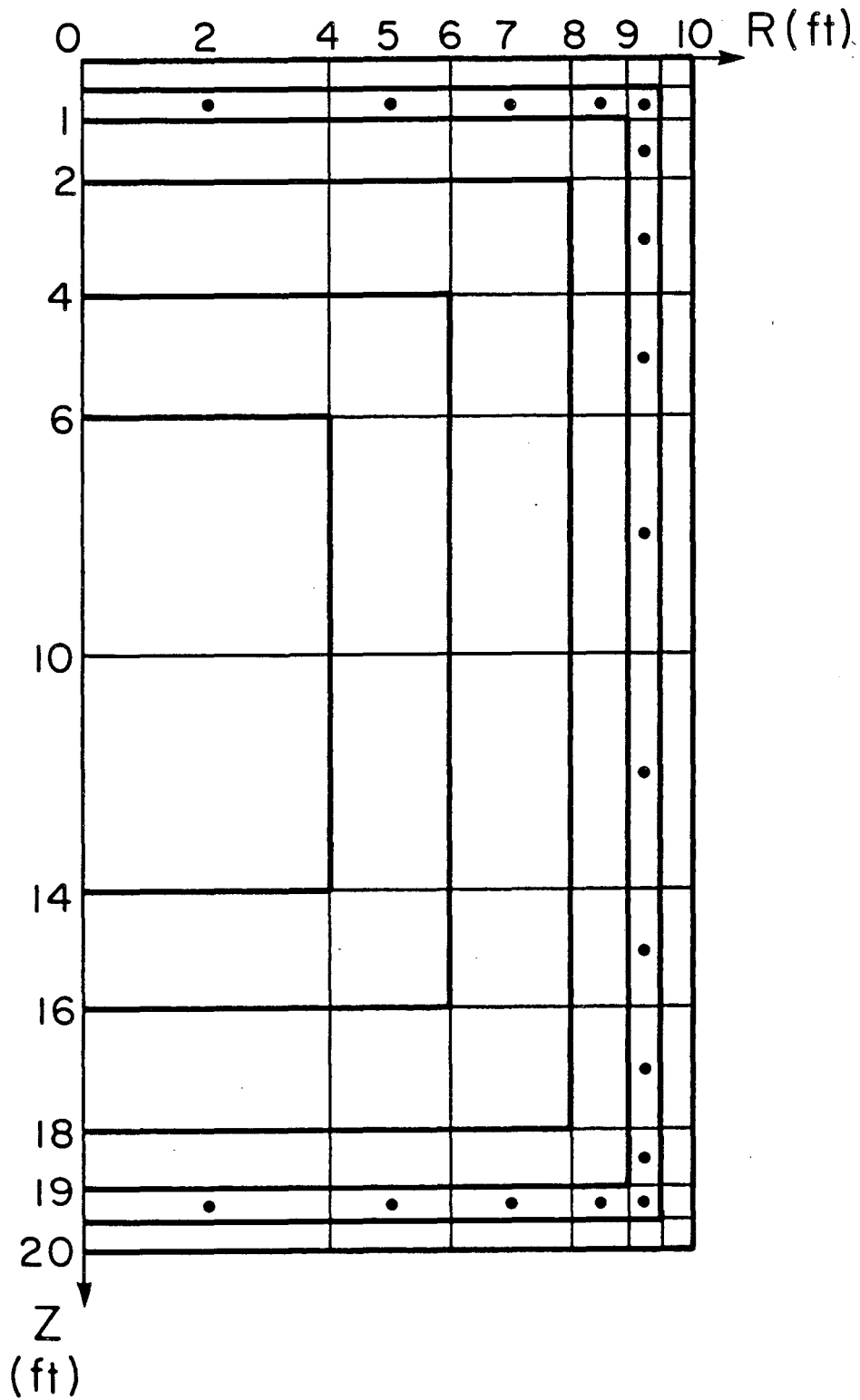


XBL 8512-12640



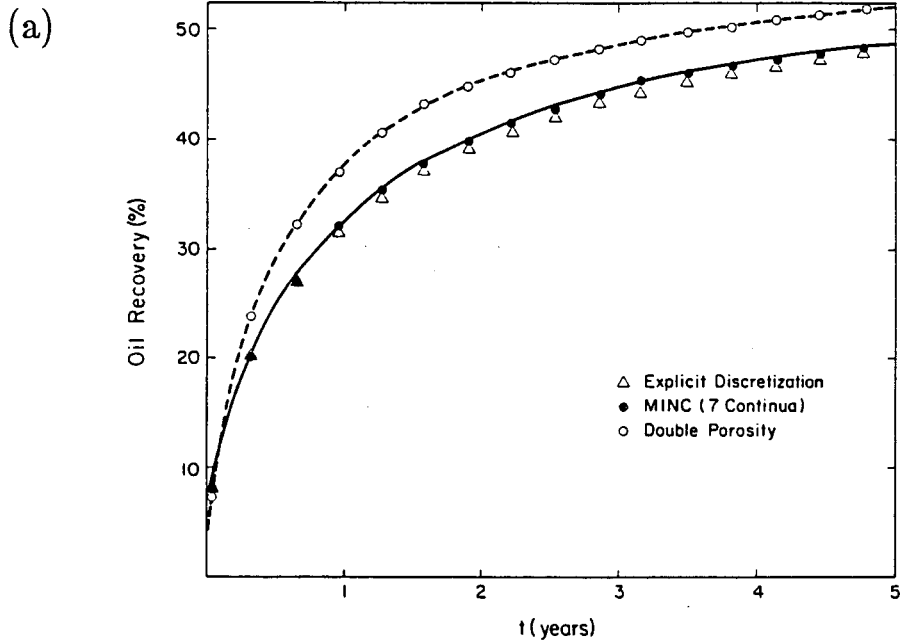
XBL 8512-12697

Fig. 1. Discretization of matrix blocks (schematic) (a) MINC, (b) Double porosity, (c) Explicit discretization.

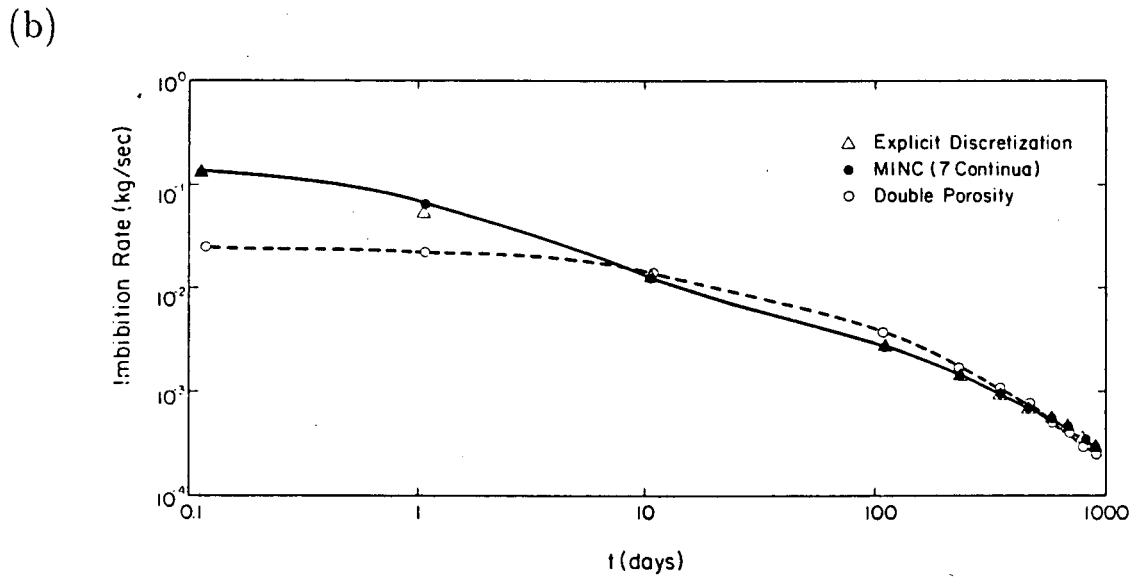


XBL 857-10609

Fig. 2. Discretization of a cylindrical matrix block for MINC and EDM.

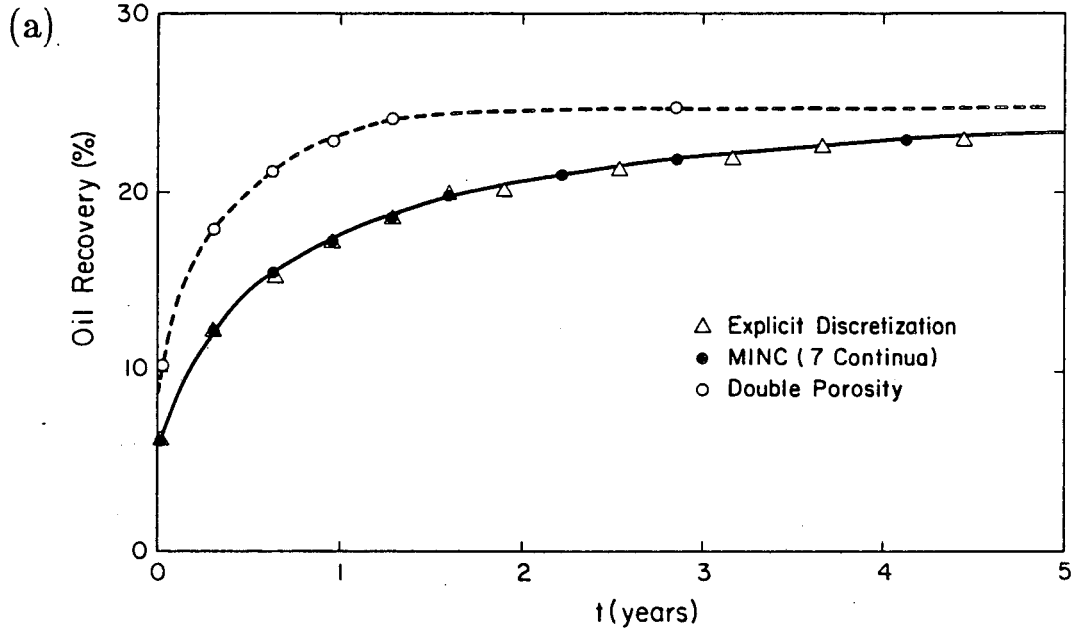


XBL 857-10601

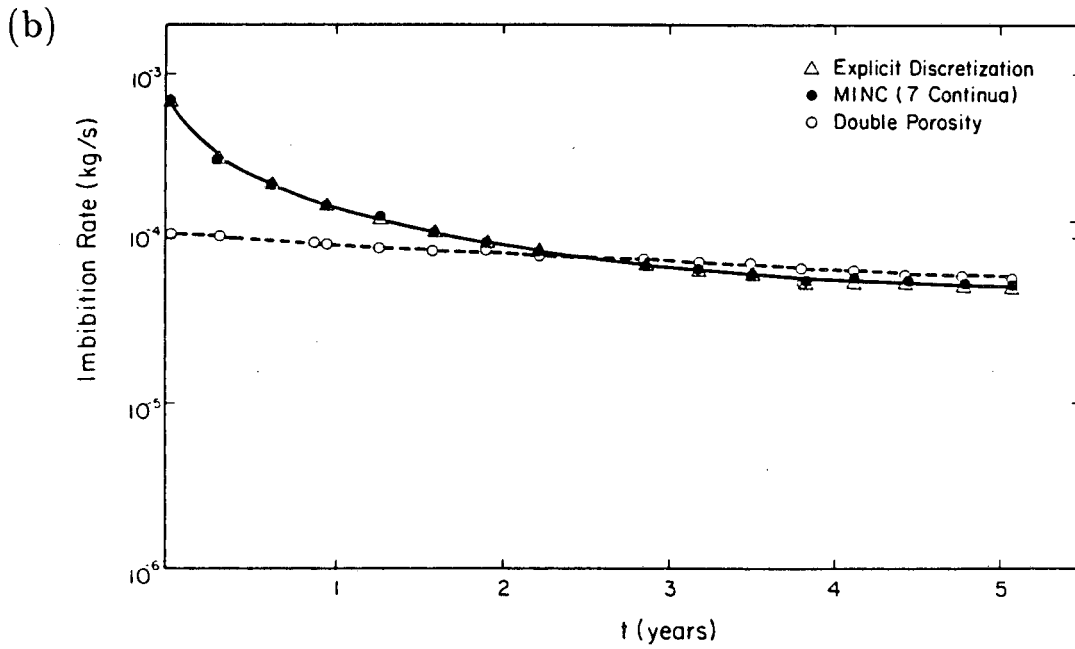


XBL 856-10600

Fig. 3. Imbibition recovery and rate from a cylindrical matrix block (Kazemi et al. data)
(a) Imbition recovery, (b) Imbibition rate.

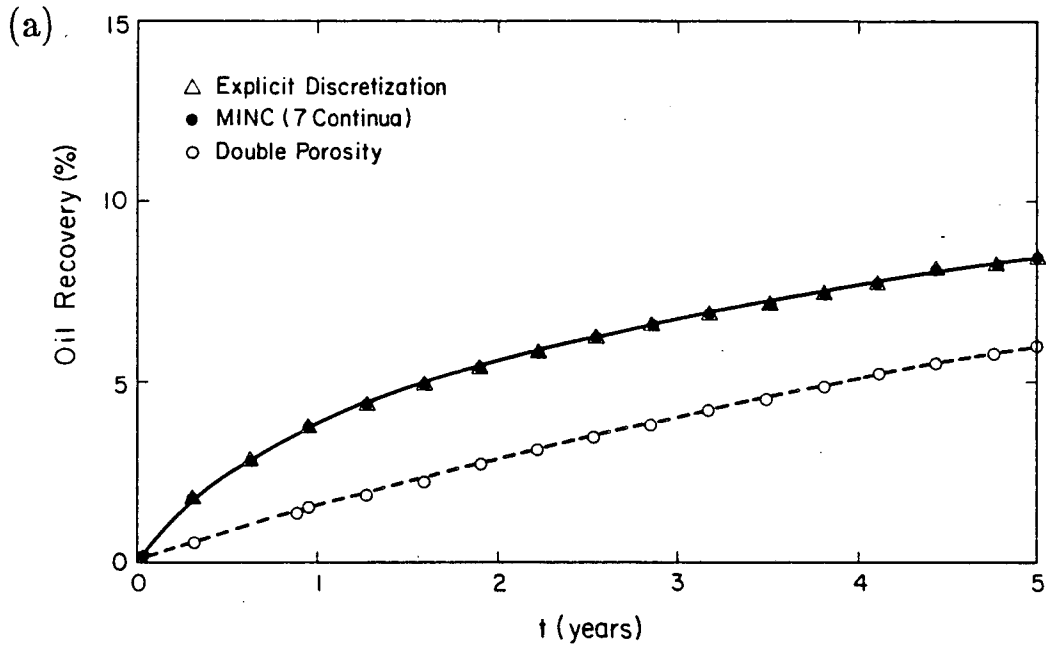


XBL 857-10605

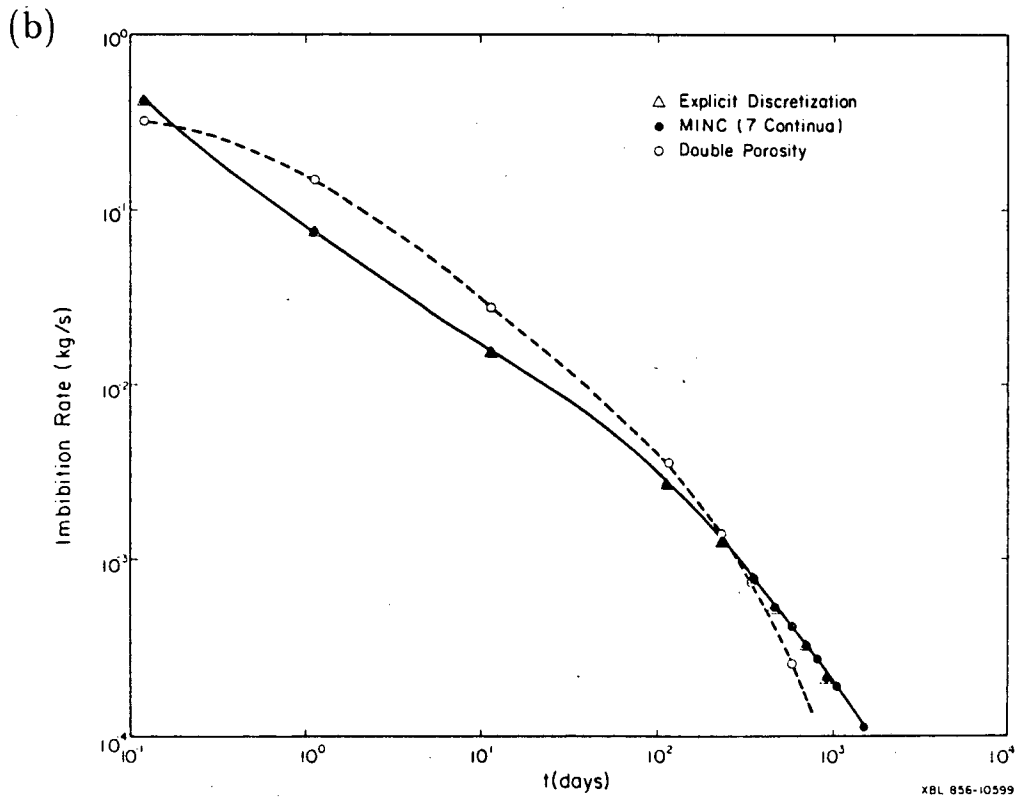


XBL 856-10598

Fig. 4. Imbibition recovery and rate from a cylindrical matrix block (Thomas et al. data)
(a) Imbibition recovery, (b) Imbibition rate.

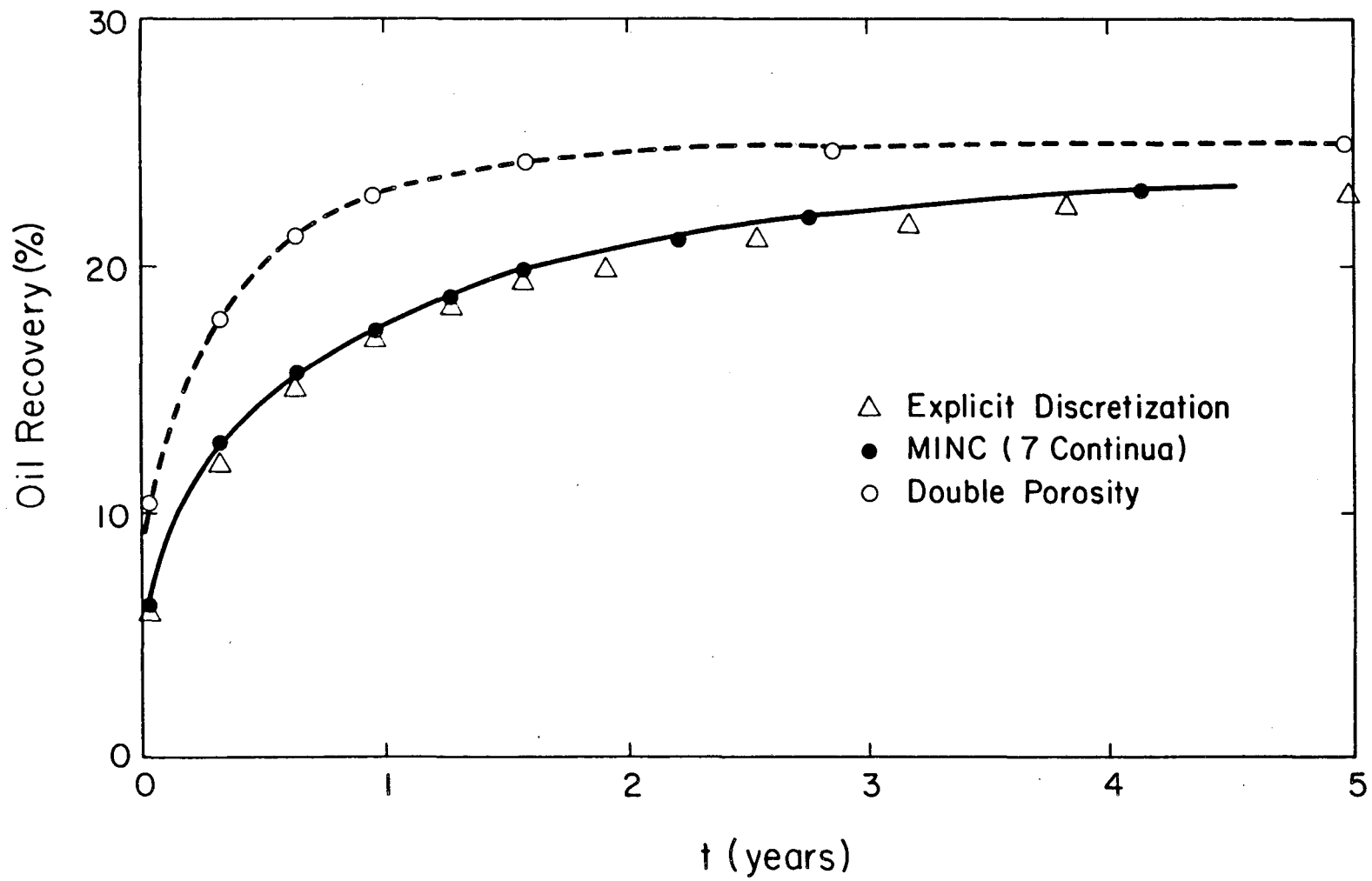


XBL 857-10604



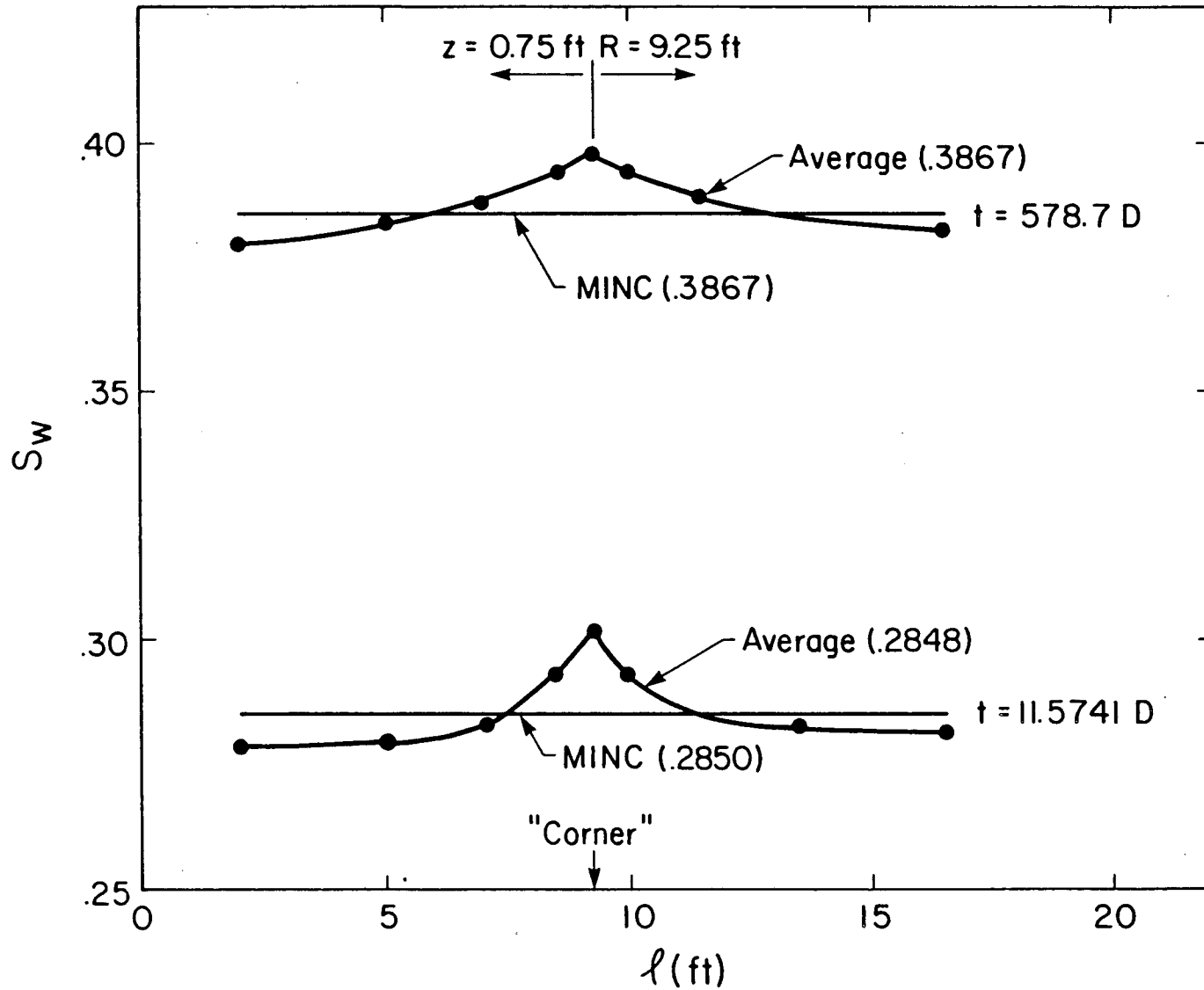
XBL 856-10599

Fig. 5. Imbibition recovery and rate from a cylindrical matrix block (Southern California Field) (a) Imbibition recovery, (b) Imbibition rate.



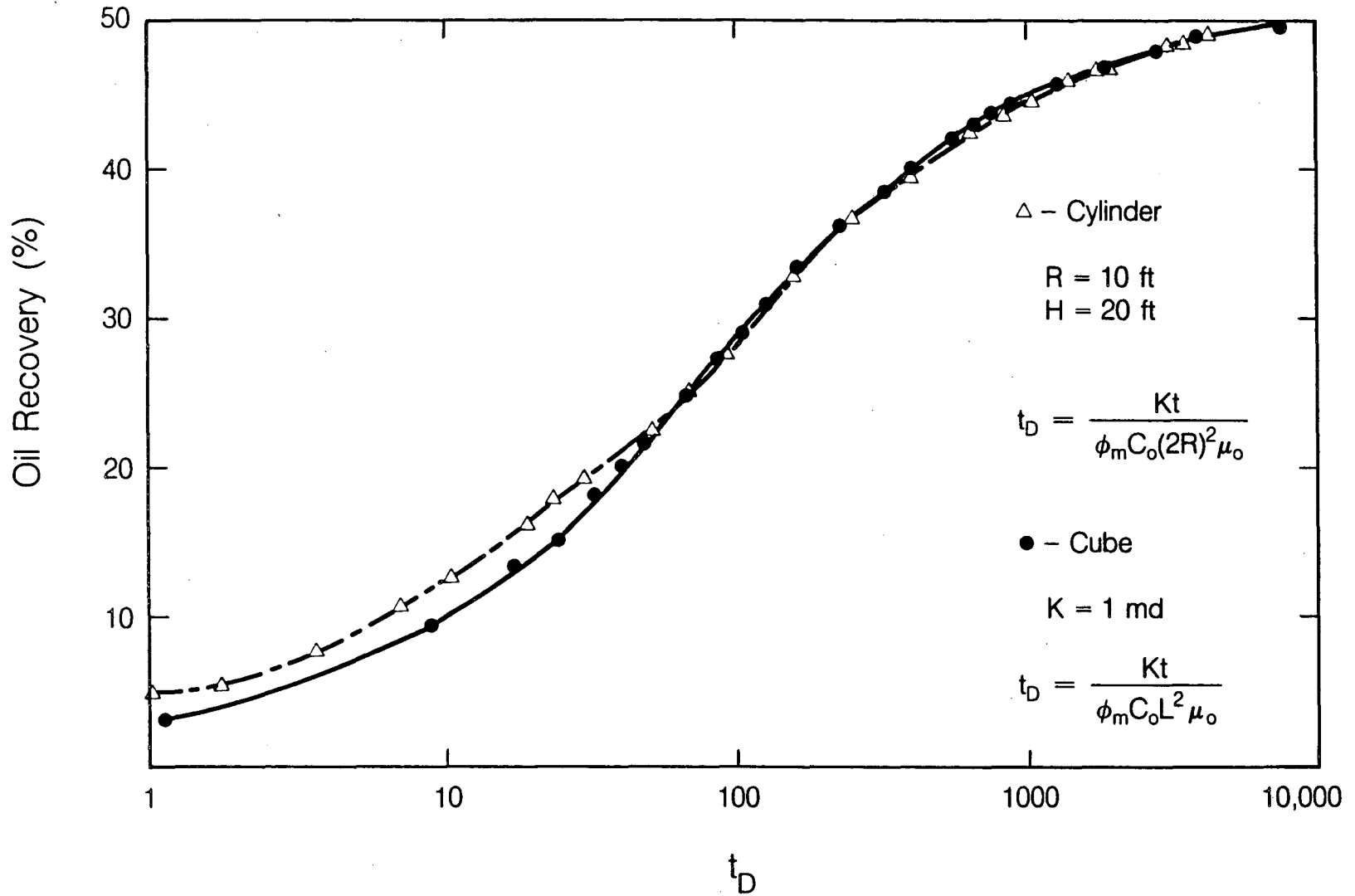
XBL 857-10607

Fig. 6. Imbibition recovery from a cubic matrix block (Thomas et al. data).



XBL 857-10608

Fig. 7. Saturation distribution in a cylindrical matrix block.



XBL 8512-12699

Fig. 8. Effect of matrix block size and rock absolute permeability on imbibition oil recovery versus dimensionless time.

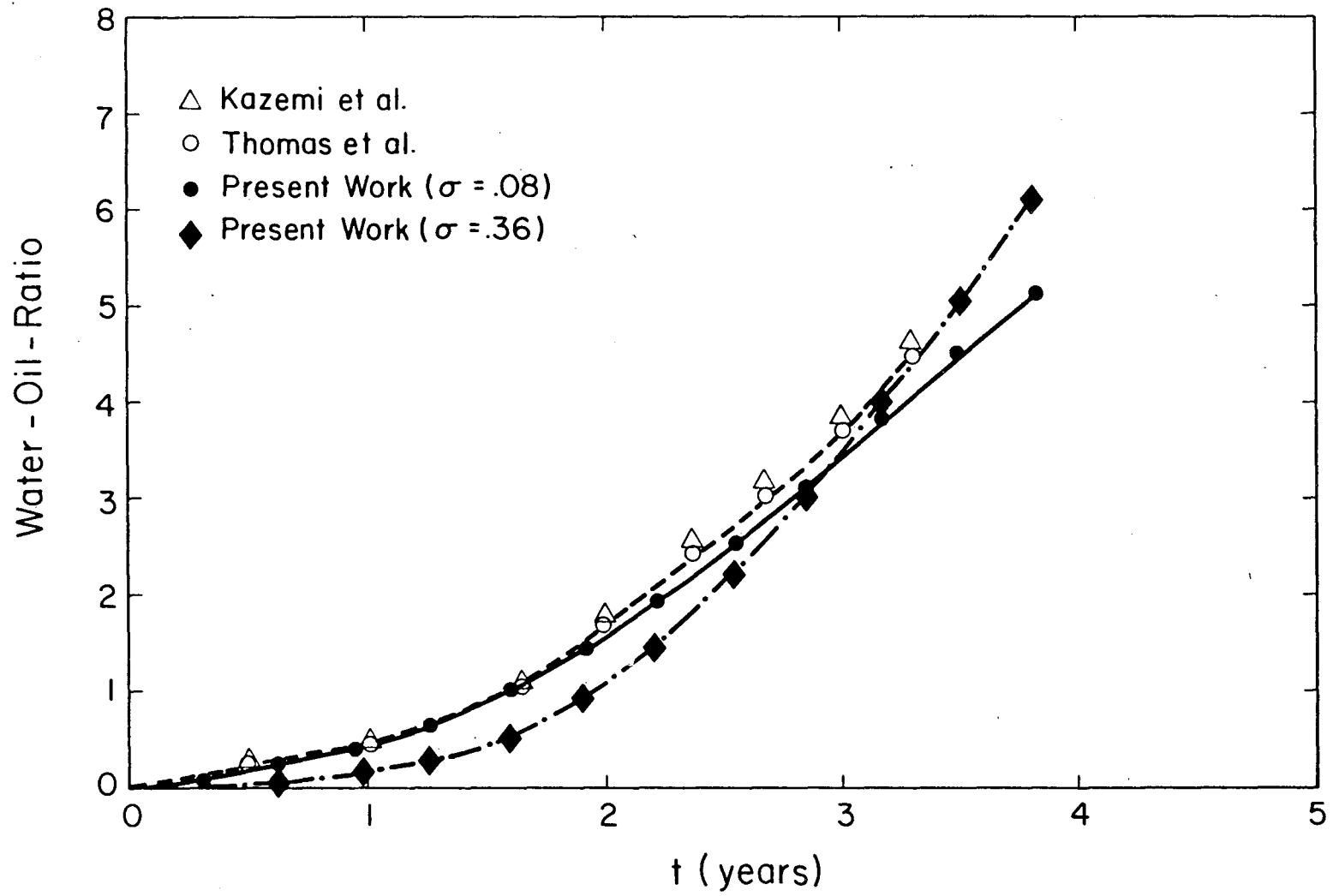
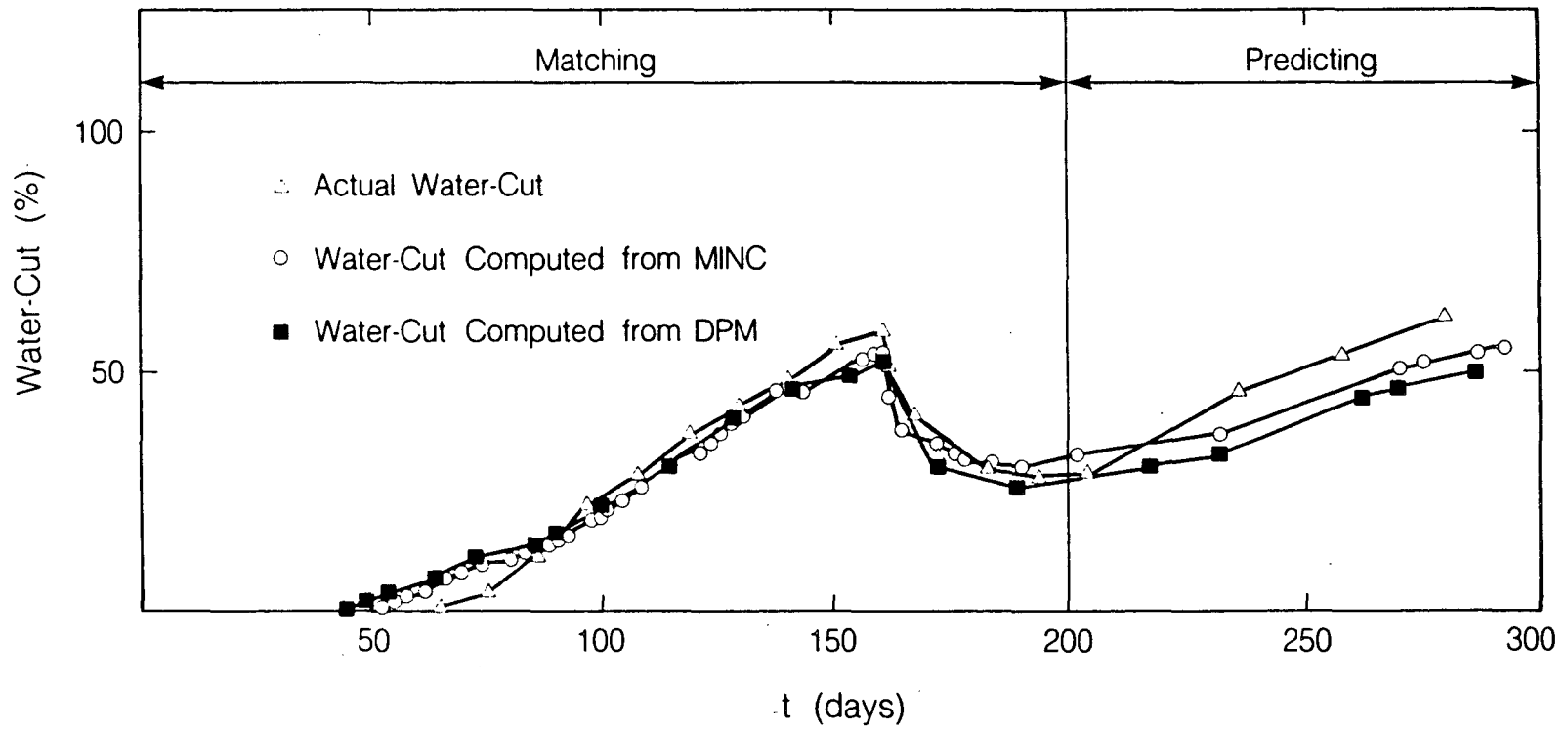


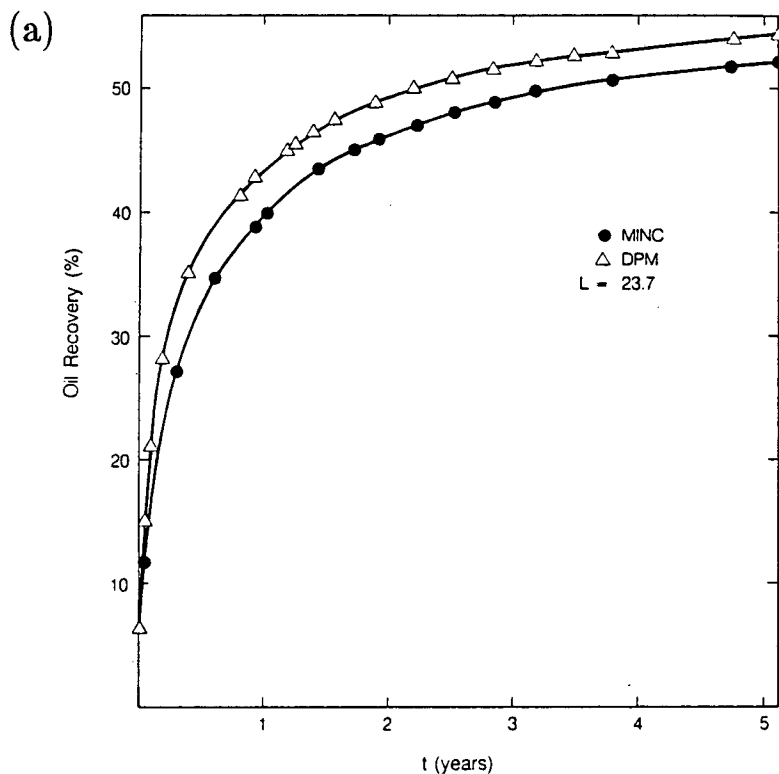
Fig. 9. Kazemi's five-spot example.

XBL 857-10606

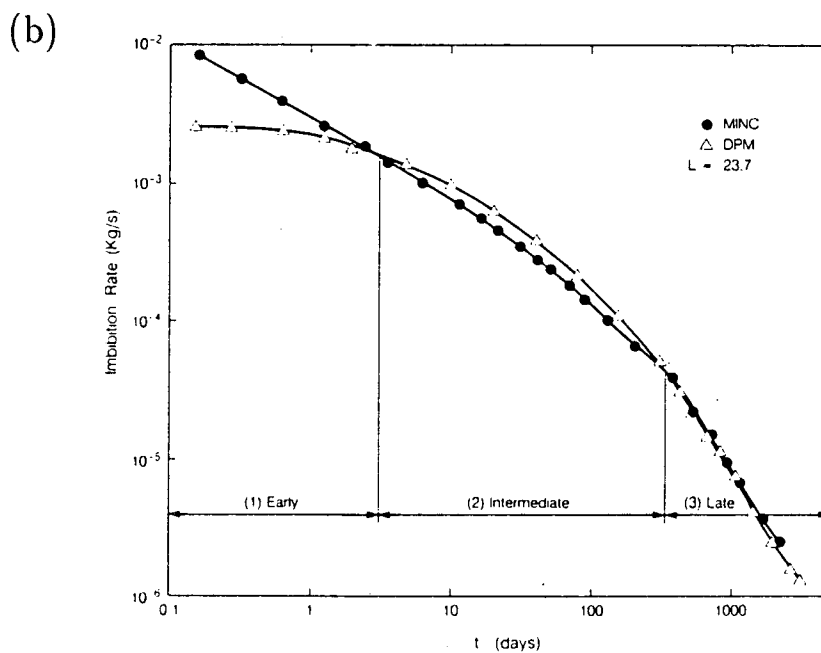


XBL 861-10503

Fig. 10. Chen's coning problem.

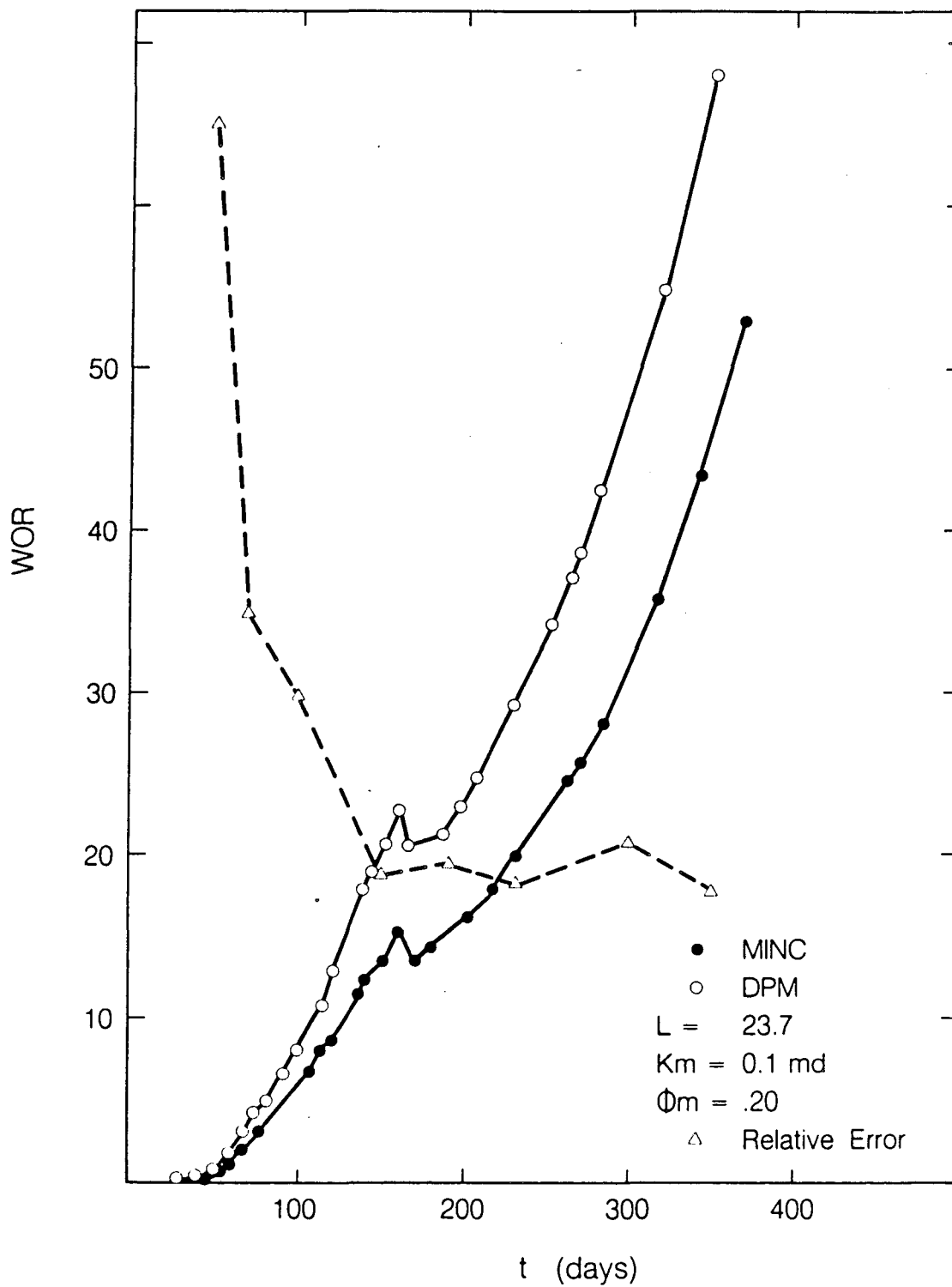


XBL 861-10496



XBL 861 10502

Fig. 11. Imbibition recovery and rate from a cubic matrix block (Chen's data) (a) Imbibition recovery (b) Imbibition rate.



XBL 861-10501

Fig. 12. Comparison of WOR from MINC and DPM (modified Chen's data).

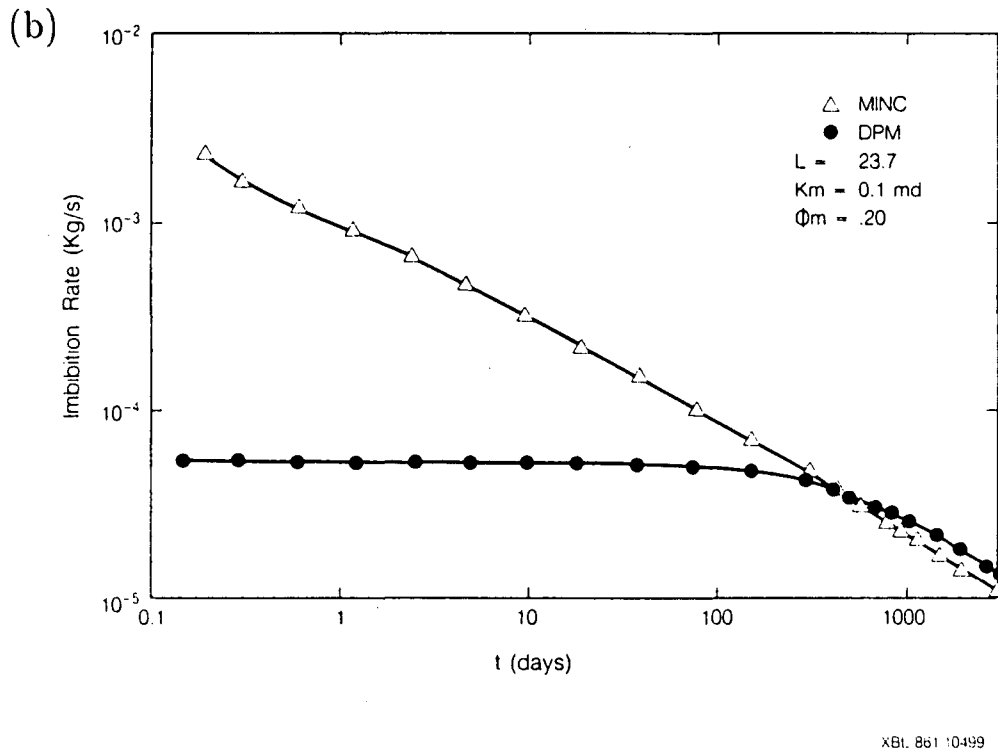
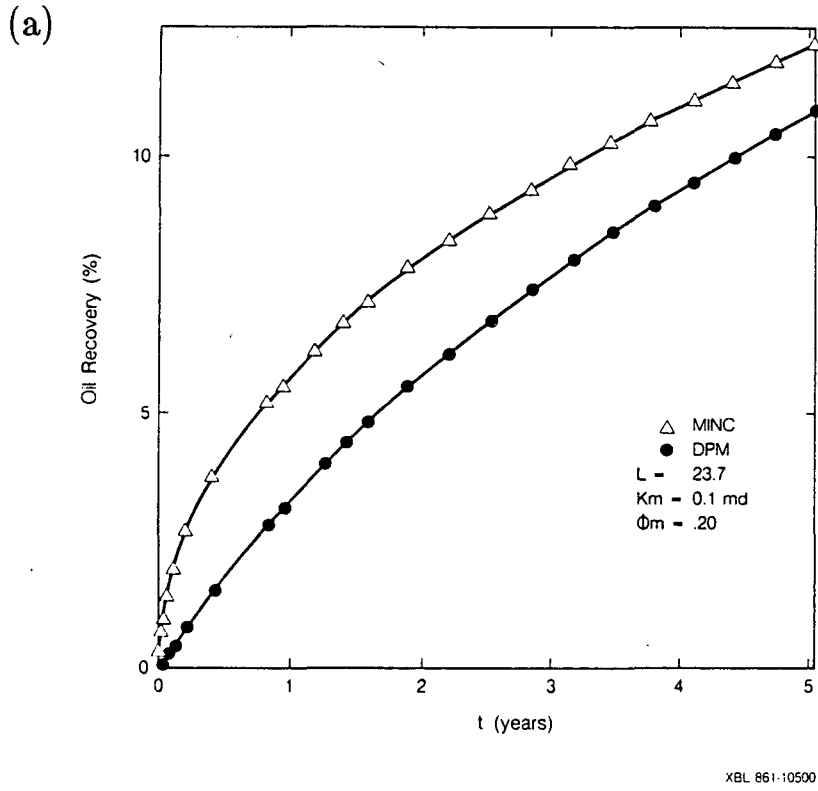
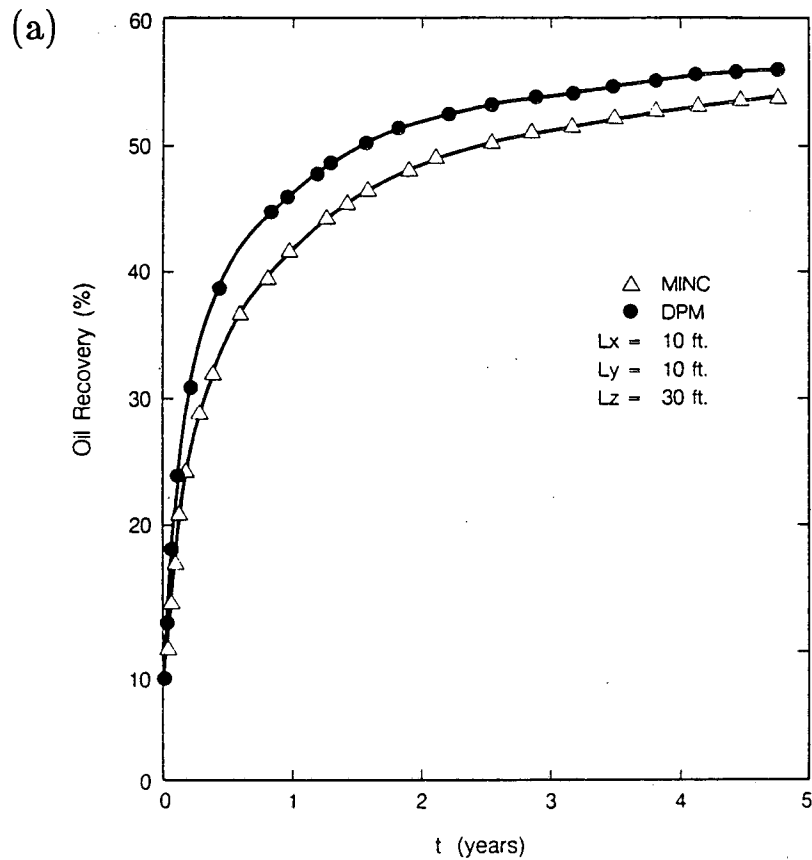
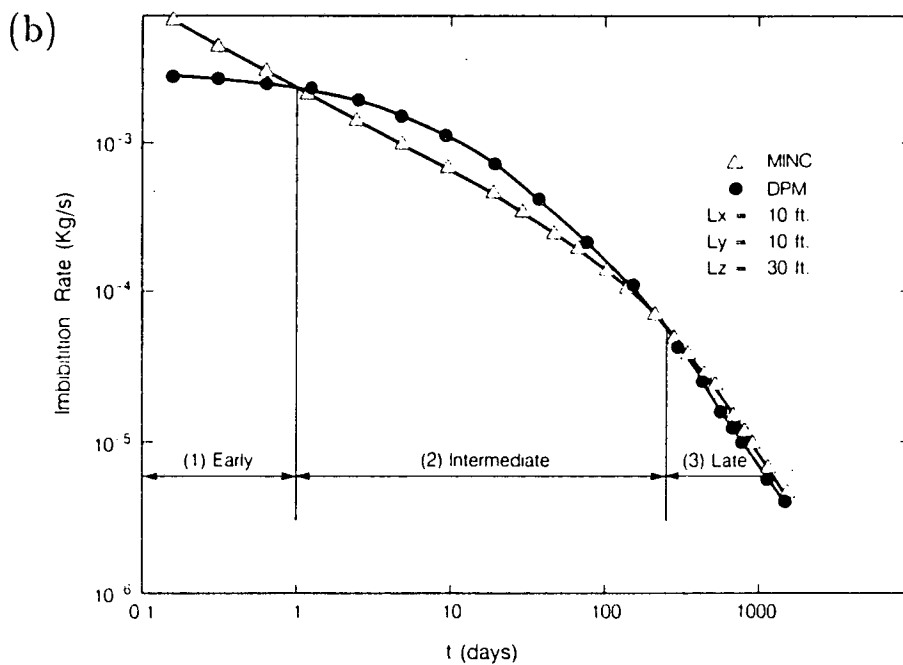


Fig. 13. Imbibition recovery and rate from a cubic matrix block (modified Chen's data)
(a) Imbibition recovery, (b) Imbibition rate.

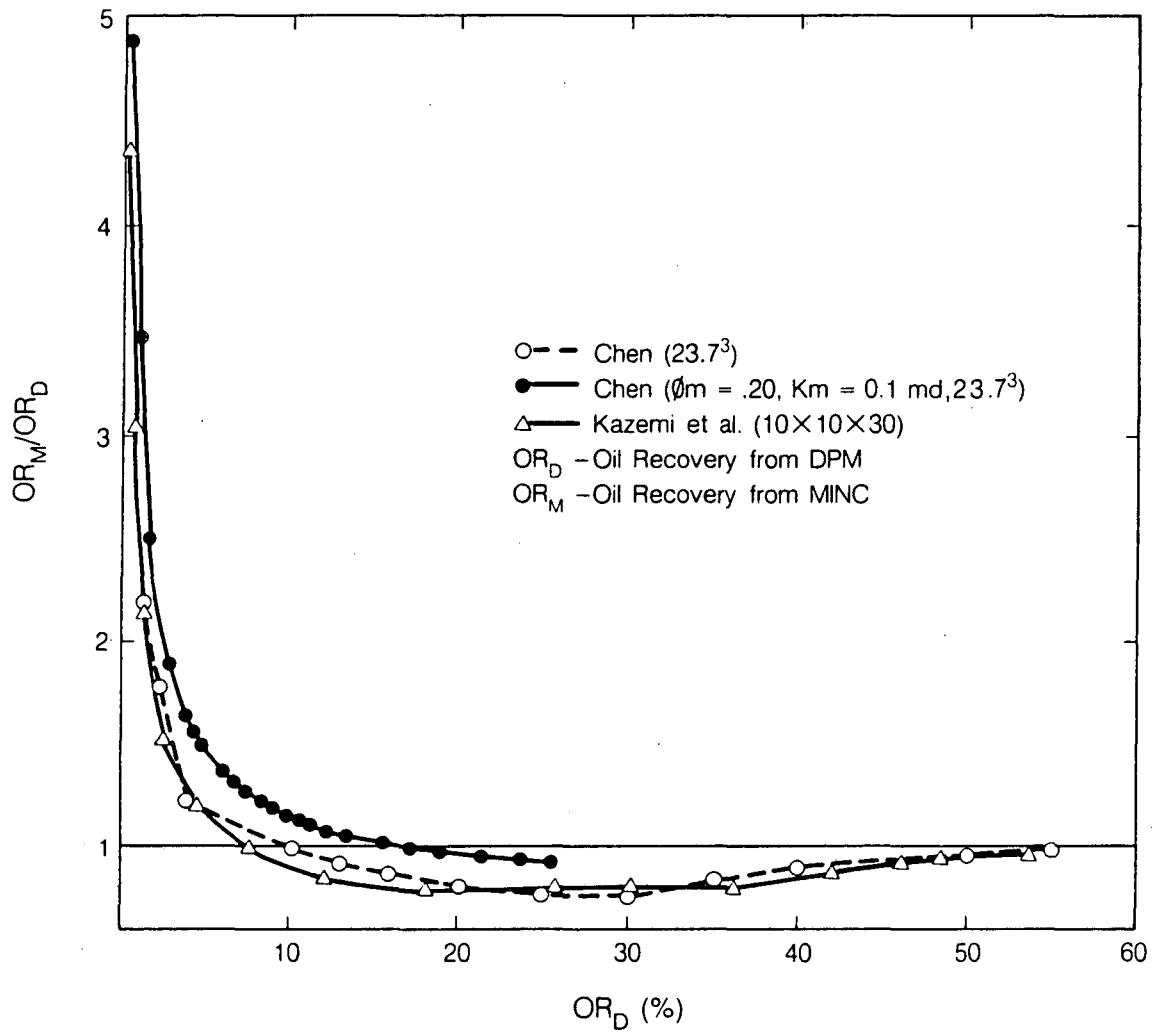


XBL 861-10498



XBL 861 10497

Fig. 14. Imbibition recovery and rate from a rectangular matrix block as used in five-spot example (a) Imbibition recovery, (b) Imbibition rate.



XBL 861-10495

Fig. 15. Comparison of imbibition oil recovery from MINC and DPM.

This report was done with support from the Department of Energy. Any conclusions or opinions expressed in this report represent solely those of the author(s) and not necessarily those of The Regents of the University of California, the Lawrence Berkeley Laboratory or the Department of Energy.

Reference to a company or product name does not imply approval or recommendation of the product by the University of California or the U.S. Department of Energy to the exclusion of others that may be suitable.

*LAWRENCE BERKELEY LABORATORY
TECHNICAL INFORMATION DEPARTMENT
UNIVERSITY OF CALIFORNIA
BERKELEY, CALIFORNIA 94720*